Applied Clay Science xxx (2015) xxx–xxx

Contents lists available at ScienceDirect

Applied Clay Science

journal homepage: www.elsevier.com/locate/clay

Research paper

Shear-thinning behaviour of dense, stabilised suspensions of plate-like particles. Proposed structural model.

J.L. Amorós [a], E. Blasco [a], V. Beltrán [b]

[a] Instituto de Tecnología Cerámica, Asociación de Investigación de las Industrias Cerámicas, Spain
[b] Department of Chemical Engineering, Universitat Jaume I, Campus Universitario Riu Sec, 12006 Castellon, Spain

A R T I C L E I N F O

Article history:
Received 17 February 2014
Received in revised form 1 June 2015
Accepted 4 June 2015
Available online xxxx

A B S T R A C T

A structural model was developed to describe the shear-thinning behaviour of dense, stabilised suspensions of plate-like particles. The model is based on the following main assumptions: the particles are distributed in more or less compact layers, oriented parallel to the flow; the particles are assumed to behave as hard disks, disk thickness being the sum of crystal thickness plus twice the Debye length; when the shear stress increases, the orientation of the plate-like particles in the flow direction also increases, thus increasing layer compactness. In order to test the proposed model, a kaolin was selected and characterised. The kaolin was used to prepare more than 40 aqueous suspensions, modifying the solids volume fraction between $\phi = 0.20$ and $\phi = 0.475$ and the dispersant (sodium silicate) content between $X_s = 0.075$ and $X_s = 0.225$ mg dispersant/m^2 solid. The flow curves of all suspensions were determined in the quasi-steady state. The results confirmed the validity of the model to satisfactorily describe the combined effect of ϕ and X_S on the flow curves in the shear-thinning range.

1. Introduction

Certain technologies used to refine and improve the industrial properties of kaolins (such as modern wet processing) and most practical applications of kaolins (such as the processing of ceramics or paper) need highly concentrated, stable kaolin dispersions with controlled rheological properties. To prepare homogeneous suspensions of kaolin with up to 70% (w/w) solids, anionic dispersants, mainly involving silicates, polyphosphates, and polyacrylates, are added (Bergaya et al., 2006).

The rheological behaviour of dense suspensions of plate-like particles is very complex, even for well-stabilised dispersions. In fact, it was verified in a previous paper (Amorós et al., 2010) that the flow curves of electrostatically well-stabilised, highly concentrated kaolin dispersions exhibit a shear-thinning segment that is sometimes followed by a shear-thickening segment. Although much theoretical and experimental work has been done, no theory currently appears fully able to predict the evolution of the flow curves with volume fraction in the case of anisotropic particles (Philippe et al., 2013). For colloidal hard spheres, the first and one of the most appropriate ways to calculate the effective hard sphere diameter was the Barker–Henderson model, based on the perturbation theory for fluids, developed in the 1960s (Barker and Henderson, 1967) (Barker and Henderson, 1976). Subsequently, various authors (Russel and Gast, 1986) (Krieger, 1972) (Beenakker, 1984) (De Kruif et al., 1985) have consequently advocated the use of effective approaches to link suspension viscosity and volume fraction. In that context, in previous papers (Amorós et al., 2010) (Amorós et al., 2012), the rheological properties of well-stabilised dispersions of kaolin were interpreted by considering the thickness of the plate-like particle with its ionic double layer as an effective thickness. The effective volume fraction of the dispersions, calculated from the ionic strength of the resulting solutions and the average thickness of the clay mineral particles, described well the combined effect of the solids volume fraction and the dispersant additions on dispersion rheological properties such as plastic viscosity and extrapolated yield stress, both determined by applying the Bingham model, or the storage modulus and the loss (or damping) factor, both determined in a linear viscoelastic regime.

Some authors (Philippe et al., 2013) (Michot et al., 2009) (Paineau et al., 2011) (Bihannic et al., 2010), adapting Quemada's equation (Quemada, 1977) (Quemada, 1998) for hard spheres to the case of disk-like particles (natural swelling clay minerals), were able to rationalise the evolution with size and volume fraction of viscosity, at different shear stresses. In this approach, the effective volume fraction accounts for the fluid volume trapped by the particles through their average motion, which depends on the volume fraction of spheres with excluded volume encompassing the particle, and an orientation parameter, which depends on shear stress. In fact, as shear stress increases, the confinement of the particles along the velocity streamlines also increases, "shrinking" the effective volume of the particles. This interpretation is in agreement with the strong shear-thinning behaviour of dense, well-stabilised suspensions of plate-like particles.

The structural model developed in the present paper is based on an idealised structure in which the particles form more or less compact

E-mail address: encarna.blasco@itc.uji.es (E. Blasco).

http://dx.doi.org/10.1016/j.clay.2015.06.011
0169-1317/

layers, oriented to the flow. The variable selected to characterise the structure of the dispersion is the ratio of the average interlayer distance to the effective thickness of the plate-like particles. This dimensionless variable, which determines the relative viscosity of the suspension, can be related to the effective volume fraction (used in previous papers (Amorós et al., 2010; Amorós et al., 2012)) and layer compactness by geometrical arguments. The effect of shear stress on relative viscosity, in this model, is quantified by the evolution of layer compactness with shear stress. Thus, when the shear stress increases, the plate-like particles become more oriented in the flow direction, increasing layer compactness and the dimensionless interlayer distance.

In order to test the proposed model, a kaolin was selected and characterised. The kaolin was then used to prepare more than 40 aqueous suspensions, modifying the solids volume fraction between $\phi = 0.20$ and $\phi = 0.475$ and the dispersant (sodium silicate) content between $X_s = 0.075$ and $X_s = 0.225$ mg dispersant/m^2 solid. The flow curves of all suspensions were determined in the quasi-steady state.

2. Development of the structural model to obtain the relationship between the flow curves, ϕ, and X_S, for dense, stabilised dispersions

2.1. Relationship between suspension viscosity (η), ϕ and X_S at constant shear stress (σ)

A structural model was used, based on the following assumptions:

i) At high shear rates, $\dot{\gamma}$, it may be assumed, in a first approach, that the plate-like particles are oriented parallel to the flow, forming compact layers (Fig. 1). For this structure:

$$\frac{h}{e} = \frac{V_{total} - V^{p}_{layer}}{V^{p}_{layer}} = \frac{\phi^{p}_{layer} - \phi}{\phi} \tag{1}$$

where V_{total} and V^{p}_{layer} are the volumes of the suspension and the particle layer, h is the interlayer distance and ϕ and ϕ^{p}_{layer} are the solids volume fractions of the suspension and the layer, respectively.

ii) It is assumed that the kaolin particles behave as thin disks, of identical thickness, "e", with diameters that display a wide distribution (Fig. 1), as a result of which the compactness of the ordered layer, $\phi^{p}_{max} = \phi^{p}_{layer}$, can reach a value of 0.9 (Qazi et al., 2010). The ratio of the average inter-particle separation, "h", to thickness, "e", or the dimensionless average distance, h*, then becomes:

$$h* = \frac{h}{e} = \frac{\phi^{p}_{max} - \phi}{\phi}. \tag{2}$$

iii) In view of the pronounced effect of the inter-particle dimensionless average separation distance, h*, on suspension viscosity (analogous to that of ϕ on η) (Amorós et al., 2010) (Quemada, 1998) (Amorós et al., 2002), the following expression was chosen to describe this effect:

$$-\frac{d\ln\eta}{dh^*} = -\frac{d\eta}{\eta dh^*} = B\frac{1}{(h^*)^2} \tag{3}$$

where B is the proportional coefficient.

When infinite dilution is taken as boundary condition, i.e. when

$$\phi \to 0, h^* \to \infty, = \tag{4}$$

where μ is the viscosity of water.

Integrating Eq. (3) with boundary condition (4) yields:

$$\eta_R = \frac{\eta}{\mu} \cdot \exp\left(\frac{B}{h^*}\right). \tag{5}$$

This equation also obeys the divergence condition, i.e. for $h^* = 0, \eta = \infty$.

Substituting Eq. (2) into Eq. (5) then gives:

$$\eta_R = \exp\left(\frac{B \cdot \phi}{\phi^{p}_{max} - \phi}\right). \tag{6}$$

iv) If it is assumed that the orientation of the particles to the flow is not completely parallel, which is what generally occurs, including at high shear stresses (Philippe et al., 2013) (Bihannic et al., 2010) (Fig. 2), using the same geometric arguments as in i), one obtains:

$$\frac{h}{c} = \frac{\phi_{layer} - \phi}{\phi} \tag{7}$$

where "c" is the layer thickness, which is always greater than "e", the particle thickness, and ϕ_{layer} is its volume fraction, which is always smaller than ϕ^{p}_{max}, corresponding to the compact layer.

Thus, by geometry, the following is obeyed:

$$\frac{c}{e} = \frac{\phi^{p}_{max}}{\phi_{layer}} > 1. \tag{8}$$

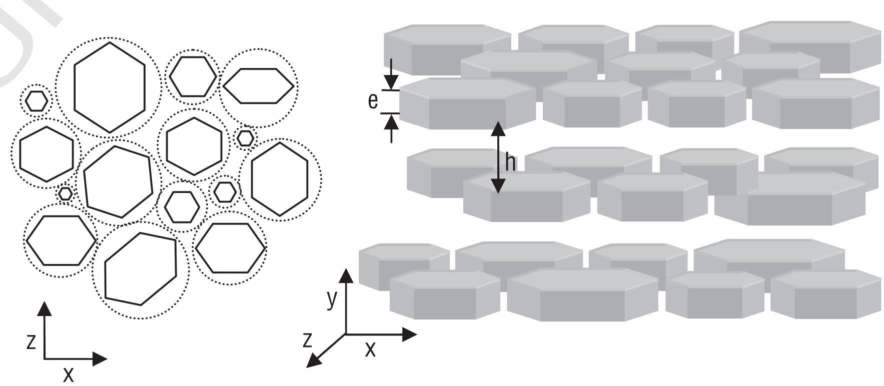

Fig. 1. Idealised structure of the kaolin suspension. Particle layers and particles entirely oriented to the flow. Flow is in the x-direction.

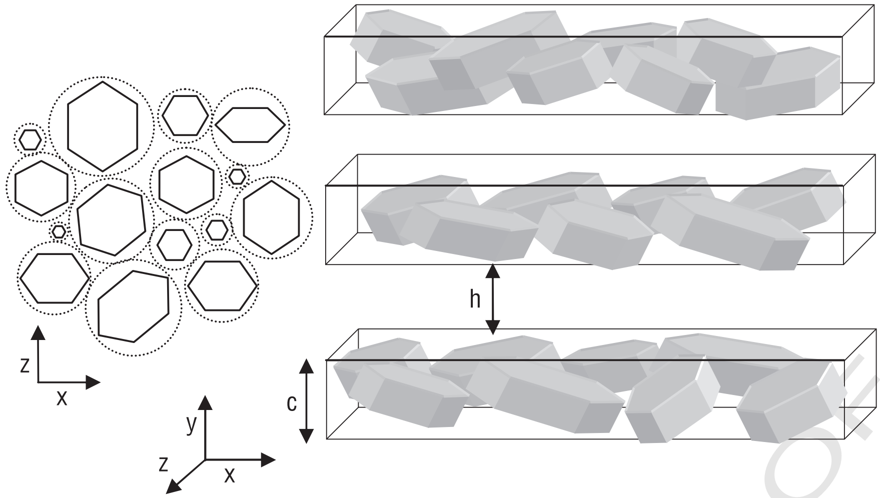

Fig. 2. Idealised structure of the kaolin suspension. Particle layers entirely, and particles partly, oriented to the flow. Flow is in the x-direction.

Eqs. (7) and (8) then yield:

$$h^{*}=\frac{h}{e}=\frac{\phi^{p}_{max}}{\phi_{layer}}\cdot\left(\frac{\phi_{layer}-\phi}{\phi}\right). \tag{9}$$

Introducing Eq. (9) in Eq. (5), and integrating using the infinite dilution boundary condition, one obtains:

$$\eta_R=\exp\left(C\cdot\frac{\phi}{1-\phi/\phi_{layer}}\right) \tag{10}$$

where $C=B/\phi^{p}_{max}$.

v) The effect of the dispersant addition, X_S, on η can be suitably described using an effective volume fraction, ϕ_{eff}, which only depends on the range of (repulsive) electrostatic interaction forces and which, therefore, regulates the minimum interparticle separation distance, as was assumed in a previous study (Amorós et al., 2010). For this purpose, the kaolinite particles are assumed to be hard disks dispersed in a fluid, which maintain their diameter, while their thickness, "e", increases from "e" to "e" plus twice the Debye length, $2\cdot\kappa^{-1}$. The effective volume fraction then becomes:

$$\phi_{eff}=\left(1+\frac{2\cdot\kappa^{-1}}{e}\right)\cdot\phi. \tag{11}$$

When the value of ϕ is replaced with that of ϕ_{eff}, and ϕ_{layer} is assumed to be a new value of ϕ^{layer}_{eff}, Eq. (10) becomes:

$$\eta_R=\exp\left(C\cdot\frac{\phi_{eff}}{1-\phi_{eff}/\phi^{layer}_{eff}}\right). \tag{12}$$

2.2. Relationship between ϕ^{layer}_{eff} and shear stress (σ)

As the shear rate, $\dot{\gamma}$, or shear stress, σ, increases in any suspension, the particles become more aligned with the flow, alignment maximising at high shear, corresponding to the minimum viscosity of the suspension. This increase in the degree of particle alignment with the flow translates into increased layer compactness, $\phi^{layer}_{eff}(\sigma)$ (Fig. 3). Consequently, a dimensionless parameter can be defined that describes the effect of shear stress, σ, on the increase in layer compactness, $\phi^{layer}_{eff}(\sigma)$, the behaviour of this parameter being similar to that of the orientation order parameter used by Egres (Egres and Wagner, 2005), or other normalised parameters used by Jogun (Jogun and Zukoski, 1999) (elastic modulus or conductivity), to study the change of particle alignment in plate-like particles (kaolin).

A degree of layer compaction, $\varphi(\sigma)$, is thus defined as:

$$\varphi(\sigma)=\frac{\phi^{layer}_{eff}(\sigma)-\phi^{layer}_{eff}(0)}{\phi^{layer}_{eff}(\infty)-\phi^{layer}_{eff}(0)} \tag{13}$$

where $\phi^{layer}_{eff}(0)$ and $\phi^{layer}_{eff}(\infty)$ are the effective solids volume fraction of the layer at low ($\sigma\to 0$) and high ($\sigma\to\infty$) shear stress (Fig. 3).

We have chosen to express $\varphi(\sigma)$ versus shear stress, σ, by a phenomenological relation:

$$\varphi(\sigma)=1-\exp\left[-\left(\frac{\sigma}{\sigma_c}\right)^{n}\right] \tag{14}$$

where σ_c and n are constant.

This relationship displays a sigmoidal dependence of $\varphi(\sigma)$ on shear stress, σ (Fig. 3). In this relationship (Eq. 14), the parameter σ_c is the shear stress value where $\varphi(\sigma)=0.63$, and n describes the shape of the curve (Fig. 3).

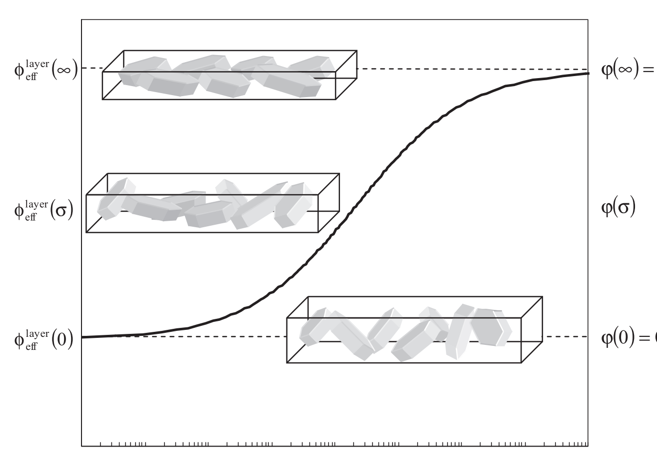

Fig. 3. Influence of shear stress, σ, on particle orientation, layer compactness, $\phi^{layer}_{eff}(\sigma)$, and the degree of layer compaction, $\varphi(\sigma)$, defined by Eq. (13).

3. Experimental

The proposed model was tested using a widely used commercial kaolin in the ceramic industry. The kaolin sample, referenced "F", was supplied by the firm AGS. The kaolin and its aqueous suspensions had already been physically and chemically characterised in a previous study (Amorós et al., 2010). Table 1 shows the chemical analysis of the kaolin, determined by X-ray fluorescence. The approximate mineralogical composition was: 5% quartz, 5% illite, 85% kaolinite, 1% sodium and potassium feldspar, 2% hematite and other iron and titanium compounds, and 2% other minerals. The specific surface area, determined by nitrogen adsorption (BET method) was 23.6 ± 0.1 m^2/g. The mean particle size, obtained from the particle size distribution, was 410 nm. The mean particle thickness, "e", obtained from the X-ray (001) reflection using the Scherrer equation, was 21 nm.

A total of 42 aqueous kaolin dispersions were prepared, changing the solids volume fraction, ϕ, from 0.20 to 0.47 and the deflocculant content, X_s, from 0.0705 to 0.225 mg dispersant/m^2 clay mineral surface area. The flow curves were determined in the quasi-steady state (Amorós et al., 2002); each flow curve required 40 pairs of shear rate–shear stress values. The secondary flow that affects these curves at high shears was corrected (Maranzano and Wagner, 2001).

In a previous study (Amorós et al., 2010) it was verified that the double layer thickness, κ^{-1}, was related to the solids volume fraction, ϕ, and to the deflocculant content, X_s, expressed in mg dispersant/m^2, by means of the equation:

$$(\kappa^{-1}) = \frac{0.68}{\sqrt{Xs}} \cdot \sqrt{\frac{1-\phi}{\phi}}. \tag{15}$$

For the studied concentrated dispersions, κ^{-1} changed from 5 nm to 1.5 nm.

4. Results and discussion

4.1. Steady-state flow curves

The flow curves, $\eta = \eta(\sigma)$, corresponding to three of the series of suspensions, each prepared with a different dispersant content, X_S, are plotted as data points (squares, circles, triangles, and diamonds) in Fig. 4. The solids volume fraction (ϕ) was modified, in each series, in the range 0.2 to 0.485.

It was verified that, independently of the value of X_S, the flow curves of all suspensions with $0.365 \le \phi \le 0.410$ exhibited a single shear-thinning segment. In contrast, at values of $\phi \ge 0.410$ the behaviour of the suspension at high shears depended on the value of X_S. Thus, at $X_S = 0.225$ mg dispersant/m^2 and high shears, the suspension was shear thickening, whereas at lower values of X_S and volume fractions above a certain value ($\phi \ge 0.46$ at $X_S = 0.135$ mg dispersant/m^2 and $\phi = 0.485$ at $X_S = 0.165$ mg dispersant/m^2), at high shears, the curve displayed a second shear-thinning segment. The shape of the flow curve resembled that of the well-known "three-region flow curve" observed in very concentrated kaolin suspensions (Moan et al., 2003). The suspensions with $\phi = 0.20$, independently of the value of X_S, were always near Newtonian.

These results confirmed the shear-thinning behaviour of electrostatically stabilised, concentrated kaolin suspensions described in the literature (Jogun and Zukoski, 1999) (Jogun, 1995) (Jogun and Zukoski, 1996). This behaviour is interpreted on the basis of the interaction between the apparent or effective volumes (exclusion effect) in concentrated suspensions of anisotropic particles such as kaolin suspensions (Jogun and Zukoski, 1999) (Jogun and Zukoski, 1996) (Moan et al., 2003) (Bossard et al., 2007). Thus, as shear ($\dot{\gamma}$ and σ) increases, the plate-like particles also increasingly align in the flow direction, reducing particle apparent volume, which ultimately translates into a decrease in suspension viscosity.

With regard to shear-thickening behaviour at high shears, the effect of solids content on the intensity of the phenomenon (positive curve slope, $\eta = \eta(\sigma)$) and on the value at which σ (flow curve minimum) began to appear was analogous to that described in other systems

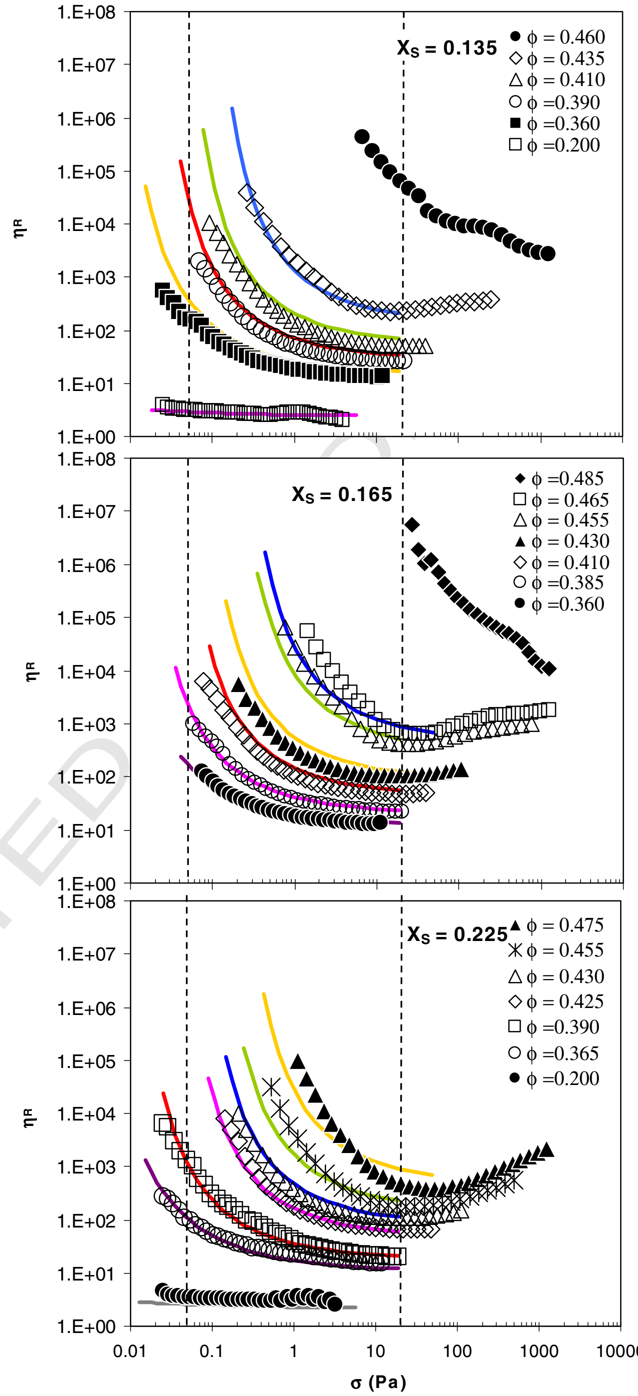

Fig. 4. Flow curves, ηR = ηR (σ). Fit of the data (solid lines) to the model (flow diagram in Fig. 7).

Table 1
Chemical analysis of clay (wt.%).

SiO_2	Al_2O_3	Fe_2O_3	TiO_2	CaO	MgO	Na_2O	K_2O	LOI[a]
47.30	36.40	1.36	1.13	0.12	0.17	0.05	0.85	12.50

[a] Loss on ignition at 1000 °C.

Please cite this article as: Amorós, J.L., et al., Shear-thinning behaviour of dense, stabilised suspensions of plate-like particles. Proposed structural model., Appl. Clay Sci. (2015), http://dx.doi.org/10.1016/j.clay.2015.06.011

(Maranzano and Wagner, 2001) (Barnes, 1989) (Boersma et al., 1990). However, the effect of deflocculant content, in particular, and of the inter-particle interaction forces, in general, on the observed shear thickening was much more complex, as shown elsewhere (Amorós et al., 2012).

4.2. Verification of the proposed structural model

The variation of $\eta_R(\sigma)$ with ϕ and ϕ_{eff}, at different dispersant contents (X_s), has been plotted, together with the fit of the results to Eq. (12), in Fig. 5. It may be observed that all values of η_R, which appeared scattered when they were plotted versus ϕ, regrouped very well in a single curve, described by Eq. 12, when they were plotted against ϕ_{eff} (Eq. 11). The values of ϕ_{eff}^{layer}, calculated for different values of σ, are detailed in Table 2. These values were obtained by fitting the data to Eq. 12, keeping C constant. The best fit was obtained by C = 1.7.

Table 2
Values of ϕ_{eff}^{layer} calculated by fitting the data to Eq. 12.

σ (Pa)	C	ϕ_{eff}^{layer}
0.05	1.7	0.52
0.1	1.7	0.54
0.5	1.7	0.57
1	1.7	0.59
5	1.7	0.61
10	1.7	0.62
20	1.7	0.62

These results confirm the validity of the developed model: on the one hand, the results fit well to Eq. 12, assuming that C is independent of σ and, on the other, ϕ_{eff}^{layer} increases with σ as the model predicts.

The values of ϕ_{eff}^{layer} and σ in Table 2 were fitted using Eqs. (13) and (14), which yielded a good correlation (Fig. 6). The values of

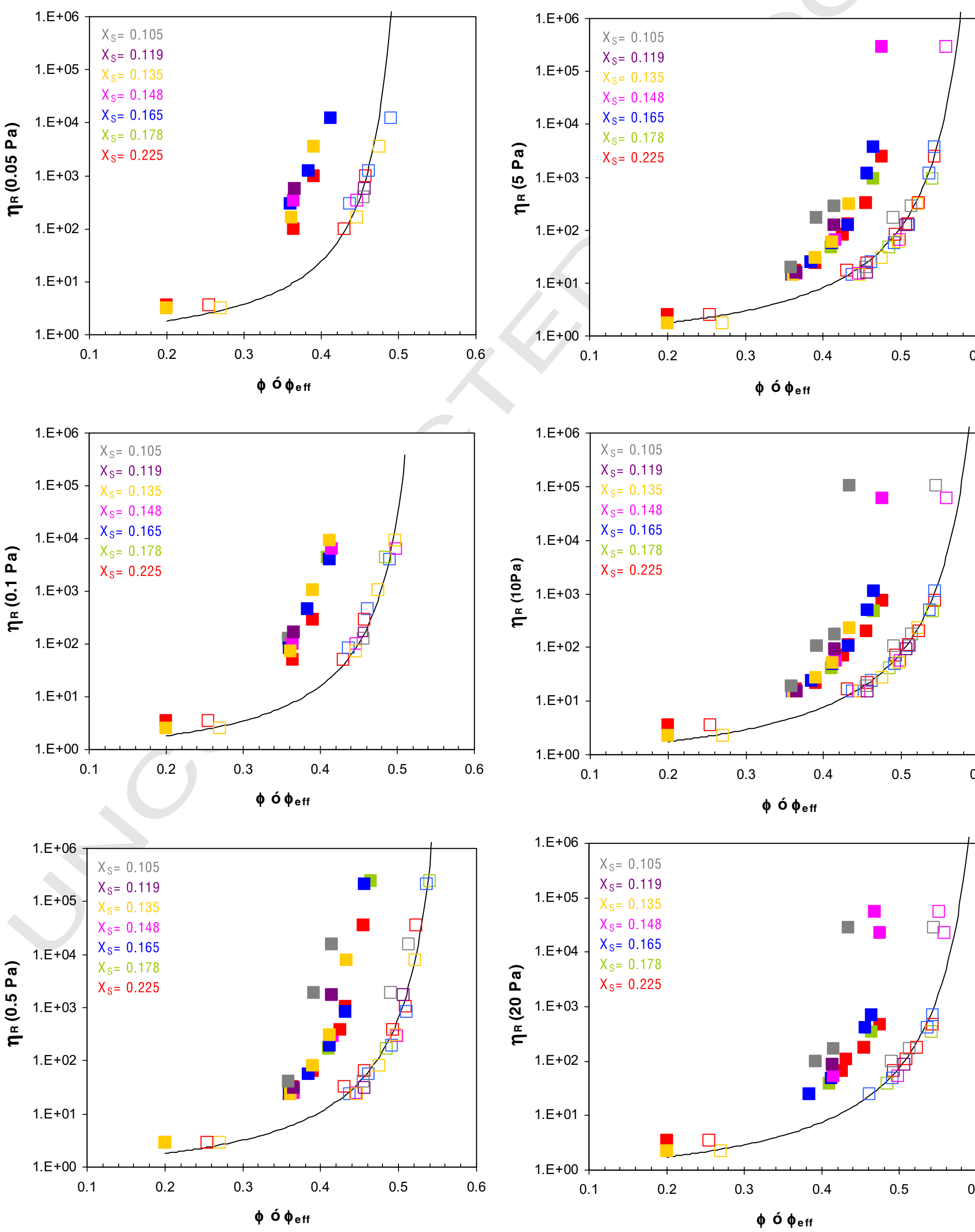

Fig. 5. Variation of ηR (σ) with ϕ (filled squares) and ϕ_{eff} (open squares) at different dispersant contents (Xs). The solid lines represent the fit of the data to Eq. (12).

Please cite this article as: Amorós, J.L., et al., Shear-thinning behaviour of dense, stabilised suspensions of plate-like particles. Proposed structural model., Appl. Clay Sci. (2015), http://dx.doi.org/10.1016/j.clay.2015.06.011

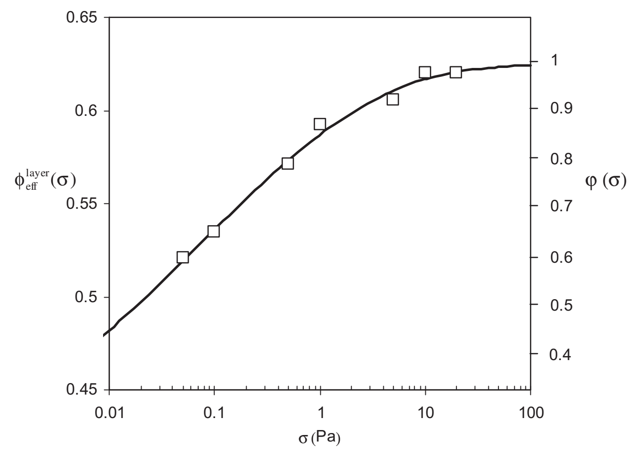

Fig. 6. Influence of shear stress, σ, on the effective layer volume fraction, $\phi_{eff}^{layer}(\sigma)$, and the degree of layer compaction, $\varphi(\sigma)$, defined by Eq. (13).

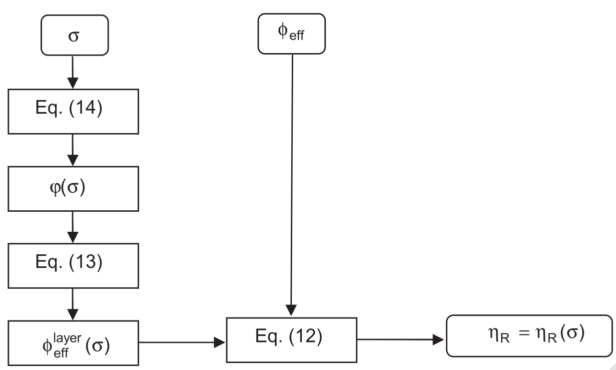

Fig. 7. Procedure followed for the reproduction of the flow curves.

the resulting fitting parameters were as follows: $\phi_{eff}^{layer}(0) = 0.36$, $\phi_{eff}^{layer}(\infty) = 0.625$, n = 0.25, and $\sigma_c = 0.07$ Pa.

Using the values of these four parameters and the measured average kaolin particle thickness e = 21 nm, and following the procedure detailed in the flow diagram in Fig. 7, the flow curves were calculated (solid curves in Fig. 4). It may be observed that the developed model satisfactorily describes the combined effect of φ and X_S on the flow curves in the shear-thinning range.

5. Conclusions

A new structural model was developed to describe the shear-thinning behaviour of dense suspensions of plate-like particles. The model is based on the following main assumptions: the particles are distributed in more or less compact layers, oriented parallel to the flow; the ratio of the average interlayer separation to the effective thickness of the plate-like particles determines the relative viscosity of the suspension; the effective thickness of the particle is the sum of the average crystal thickness plus the Debye length; when the shear stress increases, the orientation of the plate-like particles in the flow direction also increases, thus increasing layer compactness.

The flow curves of electrostatically stabilised, concentrated kaolin suspensions were determined and compared with the flow curves obtained for these suspensions using the values calculated with the proposed structural model. The results confirmed the validity of the model to appropriately describe the combined effect of the solids volume fraction and the dispersant content on the flow curves in the shear-thinning range of dense, stabilised suspensions of kaolin.

References

Amorós, J.L., Sanz, V., Gozalbo, A., 2002. Viscosity of concentrated clay suspensions. Effect of solids volume fraction, shear stress and deflocculant content. Br. Ceram. Trans. 101, 185–193.

Amorós, J.L., Beltrán, V., Sanz, V., Jarque, J.C., 2010. Electrokinetic and rheological properties of highly concentrated kaolin dispersions: influence of particle volume fraction and dispersant concentration. Appl. Clay Sci. 49, 33–43.

Amorós, J.L., Blasco, E., Orts, M.J., Sanz, V., 2012. Chapter 5. Shear-thickening behaviour of highly concentrated kaolin dispersions: Influence of particle volume fraction and dispersant concentration. Kaolinite: Occurrences, Characteristics and Applications, pp. 117–137.

Barker, J.A., Henderson, D., 1967. Perturbation theory and equation of state for fluids II. A successful theory of liquids. J. Chem. Phys. 47, 4714–4721.

Barker, J.A., Henderson, D., 1976. What is "liquid"? Understanding the states of matter. Rev. Mod. Phys. 48, 587–671.

Barnes, H.A., 1989. Shear thickening ("dilatancy") in suspensions of nanoaggregating solid particles dispersed in Newtonian liquids. J. Rheol. 33, 329–366.

Beenakker, C.W.J., 1984. The effective viscosity of a concentrated suspension of spheres (and its relation to diffusion). Physica 128, 48–81.

Bergaya, F., Theng, B.K.G., Lagaly, G., 2006. Handbook of Clay Science. Elsevier, pp. 502–506.

Bihannic, I., Baravian, C., Duval, J.F.L., Paineau, E., Meneau, F., Levitz, P., De Silva, J.P., Davidson, P., Michot, L.J., 2010. Orientational order of colloidal disk-shaped particles under shear-flow conditions: a rheological-small-angle X-ray scattering study. J. Phys. Chem. B 114, 16347–16355.

Boersma, W.H., Laven, J., Stein, H.N., 1990. Shear thickening (dilatancy) in concentrated dispersions. AIChE J. 36, 321–332.

Bossard, F., Moan, M., Aubry, T., 2007. Linear and nonlinear viscoelastic behavior of very concentrated plate-like kaolin suspensions. J. Rheol. 51, 1253–1270.

De Kruif, C.G., Van Iersel, E.M.F., Vrij, A., Russel, W.B., 1985. Hard spheres colloidal dispersions: viscosity as a function of shear rate and volume fraction. J. Chem. Phys. 83, 4717–4725.

Egres, R.G., Wagner, N.J., 2005. The rheology and microstructure of acicular precipitated calcium carbonate colloidal suspensions through the shear thickening transition. J. Rheol. 49 (3), 719–746.

Jogun, S.M., 1995. Rheology and Microstructure of Concentrated Suspensions of Plate-Shaped Colloidal Particles. B. S., Carnegie Mellon University and M. S., University of Illinois, Urbana-Champaign (Thesis).

Jogun, S.M., Zukoski, C.F., 1996. Rheology of dense suspensions of platelike particles. J. Rheol. 40, 1211–1232.

Jogun, S.M., Zukoski, C.F., 1999. Rheology and microstructure of dense suspensions of plate-shaped colloidal particles. J. Rheol. 43, 847–871.

Krieger, I.M., 1972. Rheology of monodisperse latices. Adv. Colloid Interf. Sci. 3, 111–136.

Maranzano, B.J., Wagner, N.J., 2001. The effects of particle size on reversible shear thickening of concentrated colloidal dispersions. J. Chem. Phys. 114, 10514–10527.

Michot, L.J., Baravian, C., Bihannic, I., Maddi, S., Moyne, C., Duval, J.F., Levitz, P., Davidson, P., 2009. Sol/gel and isotropic/nematic transitions in aqueous suspensions of natural nontronite clay. Influence of particle anisotropy. 2. Gel structure and mechanical properties. Langmuir 25, 127–139.

Moan, M., Aubry, T., Bossard, F., 2003. Nonlinear behavior of very concentrated suspensions of plate-like kaolin particles in shear flow. J. Rheol. 47, 1493–1504.

Paineau, E., Michot, L.J., Bihannic, I., Baravian, C., 2011. Aqueous suspensions of natural swelling clay minerals. 2. Rheological characterization. Langmuir 27, 7806–7819.

Philippe, A.M., Baravian, C., Bezuglyy, V., Angilella, J.R., Meneau, F., Bihannic, I., Michot, L.J., 2013. Rheological study of two-dimensional very anisometric colloidal particle suspensions: from shear-induced orientation to viscous dissipation. Langmuir 29, 5315–5324.

Qazi, S.J., Karlsson, G., Rennie, A.R., 2010. Dispersions of plate-like colloidal particles—cubatic order? J. Colloid Interface Sci. 348, 80–84.

Quemada, D., 1977. Rheology of concentrated disperse systems and minimum energy dissipation principle. Rheol. Acta 16, 82–94.

Quemada, D., 1998. Rheological modelling of complex fluids. I. The concept of effective volume fraction revisited. Eur. Phys. J. Appl. Phys. 1, 119–127.

Russel, W.B., Gast, A.P., 1986. Nonequilibrium statistical mechanics of concentrated colloidal dispersions: hard spheres in weak flow. J. Chem. Phys. 84, 1815–1827.

Please cite this article as: Amorós, J.L., et al., Shear-thinning behaviour of dense, stabilised suspensions of plate-like particles. Proposed structural model., Appl. Clay Sci. (2015), http://dx.doi.org/10.1016/j.clay.2015.06.011